Int. J. Pharm. Investigation, 2026; 16(3):1183-1193.
https://www.jpionline.org

Original Article

Integrative Computational Analysis of Bioactive Benzoquinones: CDK Binding, Toxicity, and Pharmacokinetics

Israa Jameel Hakeem[1], Shahnaz Haque[2], Misbahuddin Rafeeq[3], Mohammad Azhar Kamal[4], Tahani Bakhsh[5], Abdulrahman Almutairi[6], Rashed Ahmed Alniwaider[7], Ali Bin Thani[8], Qamre Alam[8,9,*]

[1]Department of Biological Sciences, College of Science, University of Jeddah, Jeddah, SAUDI ARABIA.
[2]Faculty of Medicine, Nursing and Health Sciences SEGi University and Colleges, MALAYSIA.
[3]Department of Pharmacology, Basic Medical Sciences Division, College of Medicine, Dhofar University, OMAN.
[4]Department of Pharmaceutics, College of Pharmacy, Prince Sattam Bin Abdulaziz University, Alkharj, SAUDI ARABIA.
[5]Department of Biological Sciences, College of Science, University of Jeddah, Jeddah, SAUDI ARABIA.
[6]Department of Pathology and Laboratory Medicine, King Abdulaziz Medical City, Ministry of National Guard Health Affairs (MNGHA), Riyadh, SAUDI ARABIA.
[7]Department of Pathology and Laboratory Medicine, Toxicology Laboratory, Ministry of National Guard Hospital and Health Affairs (MNGHA), SAUDI ARABIA.
[8]Department of Biology, College of Science, University of Bahrain, BAHRAIN.
[9]Department of Molecular Genomics and Precision Medicine, ExpressMed Diagnostics and Research, BAHRAIN.

ABSTRACT

Background: Cyclin-Dependent Kinase is a member of cell cycle regulatory proteins and active in the formation of tumor in breast. Three active compounds Anthraquinone, Emodin and Kaempferol are evaluated using DFT calculations, ADMET predictions, toxicity profiling, and molecular docking against CDK6 (5L2S) to predict the potential drugs against this proptien. **Objectives:** The purpose of this study was to evaluate Anthraquinone, Emodin, and Kaempferol as potential CDK6 inhibitors using integrated in silico methods (DFT, ADMET/toxicity profiling, and molecular docking). It aimed to identify the most promising scaffold by correlating electronic reactivity and binding affinity with predicted pharmacokinetic and safety profiles. **Materials and Methods:** The compounds are optimized in silico with the help of Gaussian16 suit of program and functional B3LYP with basis set 6-311G(d,p). Pharmacokinetic properties are analysed with ADMET and Binding affinity with AutoDock Vina Discovery Studio Visualizer. **Results:** FMO analysis showed that Emodin has the smallest energy gap, indicating greater reactivity, while Anthraquinone and Kaempferol are comparatively more stable. MEP maps show that oxygen atoms are key reactive sites, with Kaempferol showing the highest electronegative potential. ADMET results revealed that Anthraquinone has good BBB penetration but high carcinogenic risk and rapid clearance, Emodin shows strong oral bioavailability with mutagenicity and hepatotoxicity concerns, and Kaempferol demonstrates the longest half-life with low CNS penetration. Docking studies confirmed Emodin as the strongest binder (-9.0 kcal/mol) through hydrogen bonding and hydrophobic interactions, while Kaempferol showed moderate binding, and Anthraquinone showed strong but less favourable binding due to toxicity. **Conclusion:** Our computational approaches show that Emodin predicted as the most promising CDK6 inhibitor scaffold, Kaempferol provides balanced pharmacokinetic potential and Anthraquinone could be limited by safety risks.

Keywords: ADMET, Bioactive Compounds, Cyclin-Dependent Kinase-6 , Molecular Docking, Pharmacokinetic, Toxicity,

Correspondence:
Dr. Qamre Alam
Department of Molecular Genomics and Precision Medicine, ExpressMed Diagnostics and Research, BAHRAIN.
Email: alamqa2022@gmail.com

Received: 08-12-2025;
Revised: 12-01-2026;
Accepted: 21-04-2026.

INTRODUCTION

Cyclin-Dependent Kinases (CDKs) are a group of enzymes that add phosphate groups to other proteins, thereby regulating key cellular processes, including the cell cycle (the series of events in cell growth and division), transcription of genes (the process of making RNA from DNA), and DNA repair. Dysregulation or overactivation of CDKs is frequently observed in various cancers. This makes them attractive molecular targets for cancer

DOI: 10.5530/ijpi.20260022

Copyright Information :
Copyright Author (s) 2026 Distributed under Creative Commons CC-BY 4.0

Publishing Partner : Manuscript Technomedia. [www.mstechnomedia.com]

therapy. The search for selective and potent CDK inhibitors remains central to the development of anticancer agents. There is a continued emphasis on optimizing safety profiles (minimizing side effects) and pharmacokinetic behavior (the process by which drugs are absorbed, distributed, metabolized, and excreted in the body) (Pellarin *et al*., 2025; Ding *et al*., 2020; Lukasik *et al*., 2021).

Benzoquinones, especially 1,4-benzoquinone (p-benzoquinone) and its analogues, are organic molecules featuring two ketone groups linked by a conjugated carbon framework, which imparts significant redox activity. These molecules can undergo reversible redox cycling, repeatedly accepting and donating electrons. This process leads to the production of Reactive Oxygen Species (ROS) and the formation of covalent adducts with biological targets. Such reactivity is a double-edged sword: it underlies their observed antimicrobial and anticancer effects, but also raises concerns about cytotoxicity and off-target interactions. To better understand their therapeutic potential and limitations, electronic structure analysis utilizing parameters such as HOMO-LUMO energy gaps, charge distributions, and reactivity descriptors is essential (Mariam *et al*., 1996; Zhou *et al*., 2021; Andrades-Lagos *et al*., 2023).

Advances in computational chemistry (the use of computer simulations to model chemical structures and reactions) have enabled the integration of multiple in silico (computer-based) techniques to evaluate compounds, such as benzoquinones. Building on this foundation, studies on naphthoquinone-based molecules have employed quantum chemical calculations (mathematical methods to describe electronic structure), molecular docking (simulating how molecules bind to proteins), and pharmacokinetic modeling (ADMET, Predicting Absorption, Distribution, Metabolism, Excretion, and Toxicity) to predict biological activity and chemical stability (MH Meem *et al*., 2024; Nolan *et al*., 2025).

To translate these insights into practical applications, similar approaches have provided valuable insights into benzoquinone and naphthoquinone radical anions (negatively charged species with unpaired electrons), offering data on electron affinities (tendency to accept electrons) and vibrational properties that correlate with chemical reactivity and stability. Moreover, the utility of docking techniques is evident in studies where quinoline-based dihydrazones (nitrogen-containing small molecules) were evaluated for their binding affinity to CDK family proteins (e.g., CDK1, CDK2, CDK8), with specific attention to hydrogen bonding (attractions between hydrogen and electronegative atoms) and hydrophobic interactions (interactions involving nonpolar regions) that influence inhibitory potency (Nolan *et al*., 2025; Jia-Xing *et al*., 2025).

To systematically investigate benzoquinone derivatives as potential CDK inhibitors, a multi-step computational pipeline is proposed. The workflow begins with quantum chemical calculations using Density Functional Theory (DFT), a computational technique that studies electronic structure, to elucidate fundamental electronic characteristics, such as reactivity indices and electron distribution. Subsequently, molecular docking techniques will be employed to simulate the binding interactions between the benzoquinones and the CDK target sites, particularly the ATP-binding regions or alternative regulatory pockets. In silico ADMET and toxicity prediction tools will finally be applied, with thresholds set for acceptable ADMET properties such as oral absorption above 70%, hepatotoxicity below a defined threshold, and mutagenicity ruled out. These criteria will help in evaluating drug-likeness, pharmacokinetic suitability, and safety risks (Moussaoui *et al*., 2023; Sadeghian *et al*., 2025; Rathod *et al*., 2022)

Leverage this integrative computational strategy to pinpoint benzoquinone derivatives with strong CDK binding affinity and favorable pharmacological profiles, streamlining the discovery process for novel candidates ripe for experimental validation and therapeutic development.

MATERIALS AND METHODS

Computational Details

In this work, three compounds were examined: compound 1 (Anthraquinone), compound 2 (Emodin), and compound 3 (Kaempferol). Their molecular structures were first built using GaussView 6.1 (Roy *et al*., 2016) and then optimized with Gaussian 16 (M. J. Frisch *et al*., 2016). The calculations were carried out using the B3LYP hybrid functional (Lee *et al*., 1988; Becke *et al*., 1993) with the 6-311G(d,p) basis set (Frisch *et al*., 1984), a combination that has been widely used and shown to be reliable in previous studies (M. Sharma *et al*., 2025; T. Valarmathi *et al*., 2023; R.A. El-Kasaby *et al*., 2025). The Density of States (DOS) was obtained by using the GaussSum software (Trott *et al*., 2009).

Molecular Docking

The crystal structures of the selected proteins were retrieved from the RCSB Protein Data Bank.

In this work, the X-ray co-crystal structure of human CDK6 (PDB ID: 5L2S) (https://www.rcsb.org/structure/5L2S) was employed. Cyclin-Dependent Kinase 6 (CDK6) is an enzyme that helps regulate the growth and division of cells by working together with a protein known as cyclin D. It is involved specifically in promoting the transition from G1 phase to S phase, where DNA replication takes place. Errant CDK6 activity can result in runaway cell growth that fuels cancers such as acute myeloid leukemia, breast cancer and lymphoma. Furthermore, as a cell cycle mediator, CDK6 is also a significant target in cancer treatments, and its inhibitors are being used as potential drugs to treat cancer. The receptor grid box was set at the centre coordinates of x=25.413 Å, y=36.491 Å, z=-7.997 Å, before molecular docking

and docking simulations were carried out by AutoDock Vina (Jia-Xing *et al.*, 2025) and analyzed ligand-protein interactions with Discovery Studio Visualizer 4.0 (BIOVIA Systems Dassault, 2021) (Allouche *et al.*, BIOVIASystemes *et al.*, 2021).

ADMET

ADMET analysis, we used the ADMETlab 2.0 web server (https://admetmesh.scbdd.com) (Rathod *et al.*, 2022). ADMET refers to Absorption, Distribution, Metabolism, Excretion, and Toxicity, and serves as a key step in drug discovery since it helps in understanding both the pharmacokinetics and safety profile of compounds. Through computational predictions of these properties, it becomes possible to anticipate how effectively a compound could act as a drug candidate even before carrying out experimental studies.

RESULTS

Optimization and Frontier Molecular Orbitals

The three compounds were optimized, and their optimized structures are shown in Figure 1. According to Frontier Molecular Orbital (FMO) theory, the Highest Occupied Molecular Orbital (HOMO) and the Lowest Unoccupied Molecular Orbital (LUMO) play a crucial role in determining a molecule's reactivity and its interactions with other species. The energy difference between these orbitals strongly affects stability, reactivity, and optical behaviour, where a smaller gap usually reflects greater chemical reactivity (Xiong et ail., 2021; Krishna *et al.*, 2024).

The HOMO values for compounds 1-3 are computed to be -7.26 eV, -6.39 eV and -5.77 eV. The LUMO values for compounds 1-3 are computed to be -3.02 eV, -2.60 eV and -1.52 eV. The energy gaps for compounds 1-3 are computed to be 4.24 eV, 3.79 eV and 4.25 eV (Figure 2). he variations in the energy gaps highlight differences in electronic distribution and potential reactivity among the compounds. The relatively smaller gap in compound 2 indicates a greater ease of electronic excitation, while compounds 1 and 3, having wider gaps, are expected to be comparatively more stable but less reactive.

Density of States

The density of states plots shows the electronic structures of the three studied compounds (Figure 3). The Green line shows occupied orbitals, the red line shows unoccupied (virtual) orbitals, blue curve shows total DOS. The HOMO and LUMO levels are labelled with their energy gaps. In the compound (a), the energy gap is found to be 4.24 eV, indicating moderate stability and reactivity. Compound (b) has the smallest energy gap of 3.79 eV, suggesting it is relatively more reactive and easily excitable electronically than the others. The energy gap of compound (c) is 4.25 eV, similar to compound (a), and indicates a higher electronic stability but less reactivity than in the case of compound (b). The pronounced peaks in the DOS curves correspond with the distribution and density of molecular orbitals, and the relative positions of HOMO/LUMO also confirm the energy required for electron transfer. These plots show that compound (b) is more reactive than the other two due to its smaller band gap, where compounds (a) and (c) are more stable but have lower reactivity.

Molecular Electrostatic Potential Maps

The MEP maps of these three compounds are shown in Figure 4. The differing colours in the surfaces indicate how the electron density is distributed through each molecule. The red areas are where there is a relatively high density of electrons, which then makes it more susceptible to electrophilic attack. Conversely, the blue areas are electron-deficient and can act as nucleophilic attack sites. Green regions are sites of average electro density, which may be less polar or reactive (Gu *et al.*, 2024; Abuhejail *et al.*, 2024).

Compound 1, the MEP surfaces display a more equilibrated distribution with intermediate electron density extending in all parts of the aromatic ring. Compound 2 shows larger electron-rich areas for the oxygen atoms, indicating these positions as potential reactive sites for electrophile attack. Compound 3 presents the most significant electronegative regions, especially around its hydroxyl and carbonyl groups, accounting for higher reactivity in comparison with the other compounds. The electronegative potential values for compound 1, compound 2, and compound 3 are -4.285 e^{-2}, -7.564 e^{-2}, and -7.943 $e^{-2,}$ respectively (Figure 4). MEP maps show that compound 3 has a more negative potential than the other compounds.

The finding of more positive electronegative potential of compound 3 is confirmed by Mulliken charge distribution analysis with the presence of extremely negative partial charges for active sites, which reiterates that compound 3 processes a higher ability to attract electrons than other elements (Figure 5).

ADMET Analysis

The ADME data shows a detailed description of the pharmacokinetic behaviour of the three compounds (Table 1). Compound 1 has the lowest molecular weight (208.05 g/mol), without a hydrogen bond donor and with fewer acceptors, compared to compounds 2 and 3 which should indicate its lower polarity and lower interaction possibility. On the other hand, compound 3 (with the maximum molecular mass of 286.05 g/mol) has more hydrogen bond donors and acceptors, indicating a high possibility for intermolecular interactions. Total polar surface area (TPSA) varies from 34.14 (compound 1) to 111.13 (compound 3), suggesting improved solubility and decreased membrane penetration tendency with increasing polarity, respectively. This is further confirmed by their corresponding Log P values, in which compound 1 is lipophilic (3.414) whereas compound 3 is relatively less lipophilic (2.656). The solubility, as per Log S, is the worst in 2. Permeability predictions (Caco-2 and

Table 1: Predicted ADMET properties of the compounds 1, 2 and 3.

ADME	Compound 1	Compound 2	Compound 3
MW	208.05	270.05	286.05
H-bond acceptors	2	5	6
H-bond donors	0	3	4
Rotatable bond	0	0	1
TPSA	34.14	94.83	111.13
Log S	-5.143	-5.594	-3.624
Log P	3.414	3.856	2.656
Caco-2 Permeability	-4.631	-5.149	-4.974
MDCK Permeability	1.8×10^{-6}	1.1×10^{-6}	9×10^{-6}
Pgp-inhibitor	0.954	0.014	0.004
Pgp-substrate	0.0	0.006	0.011
HIA	0.005	0.016	0.008
$F_{20\%}$	0.007	0.82	0.856
$F_{30\%}$	0.991	0.999	0.993
PPB	98.45%	99.29%	97.86%
VD	0.821	0.482	0.522
BBB Penetration	0.145	0.056	0.009
Fu	1.416%	1.640%	4.411%
CYP1A2 inhibitor	0.962	0.95	0.972
CYP2C19 inhibitor	0.555	0.103	0.181
CYP2C9 inhibitor	0.568	0.575	0.653
CYP2D6 inhibitor	0.037	0.378	0.722
CYP3A4 inhibitor	0.199	0.651	0.697
CL	2.4	9.245	6.868
$T_{1/2}$	0.088	0.385	0.905

MDCK) indicate that compound 1 has a higher relative intestinal permeability compared to compound 3, while compound 3 showed better MDCK permeability, demonstrating improved penetration across the cell membrane. Compound 1 exhibits remarkably strong P-glycoprotein (Pgp) inhibition, whereas compounds 2 and 3 exhibit very weak Pgp inhibition, which suggests a lower risk of drug efflux for the latter two inhibitors. Concerning absorption, the Human Intestinal Absorption (HIA) values are low for all compounds and compounds 2 and 3 present a higher oral bioavailability (F20% F30%) than compound 1. PPB is high in each three, with the strongest binding to compound 2. Values of Volume Distribution (VD) or blood-brain barrier penetration show that compound 1 is distributed more extensively within tissues and also penetrates the BBB more than compounds 2 and 3.

The fraction unbound (Fu) is the greatest for compound 3, which means there is more drug-free in plasma. With respect to metabolism, all three compounds exhibit mechanisms of interaction with cytochrome P450S, with compound 3 displaying the highest inhibitory trend against CYP2D6 and CYP3A4. Last, Clearance (CL) values suggest that compound 1 is more rapidly cleared compared to compounds 2 and 3 which also coincides with its short half-life [$T_{1/2}$=0.088]) and compound 3 displays the longest half-life (0.905).

Toxicity Analysis

The toxicity of three compounds shows several differences have been observed in their safety profile (Table 2). The hERG block values are low in all three, have a low cardiotoxicity risk, although compound 3 has a slightly higher value than compounds 1 and 2. Human risk for Hepatotoxicity (H-HT) is moderate, but compound 3 presents with the highest probability (0.098). Drug-Induced Liver Injury (DILI) potential values are likely to be high for all compounds, which is very clear from the values obtained, particularly in the case of compound 3 (0.979). As for mutagenicity (measured by AMES toxicity), compound 2 is expected to be the riskiest (0.823), but compound 3 should be relatively safe (0.672). Values for rat oral acute toxicity indicate

that all the compounds are of similar toxicity level; however, compound 3 appears slightly more toxic.

Prediction of the FDA maximum recommended daily dose (FDAMDD). The predicted result of FDAMDD is also shown in Table 2, in which the compound 2 exhibits the strongest attention (0.916), while the compound 3 has its weakest concern (0.109). Concerning skin sensitization, compounds 2 and 3 appear to be more hazardous than compound 1. The carcinogenicity values suggest that compound 1 is likely to have a high potential (0.901), whereas compound 3 poses a significantly lower risk (0.097). The ocular toxicity prediction indicates a very low probability of eye corrosion for all compounds; however, compound 3 (0.009) shows a slightly increased value. The eye irritation potential for all three compounds is also high, with compound 1 being the highest (0.986). The overall risk of respiratory toxicity is low, but progressively higher from compound 1 to compound 3.

Molecular Docking

Molecular docking analysis was performed for CDK6 (5L2S) and compound 1 (Anthraquinone), compound 2 (Emodin) and compound 3 (Kaempferol). The nine docked poses of the three compounds against the target protein (5L2S) showed different binding affinities (Table 3). Compound 2 shows the most favourable and incisive binding docking scores -9.0 to -8.1 kcal/mol. Pose 1 (-9.0 kcal/mol) displays a strong and beneficial binding pattern that continues throughout the poses. Compound 1 also reveals strong binding results, contributing with docking scores ranging from -8.8 to -7.5 kcal/mol, more stable at dock poses 1 (-8.8 kcal/mol), indicating high binding site affinity interaction toward the receptor. Compound 3, in comparison, records slightly weaker interactions, with scores ranging from -8.5 to -6.9 kcal/mol, though still within a favourable binding range.

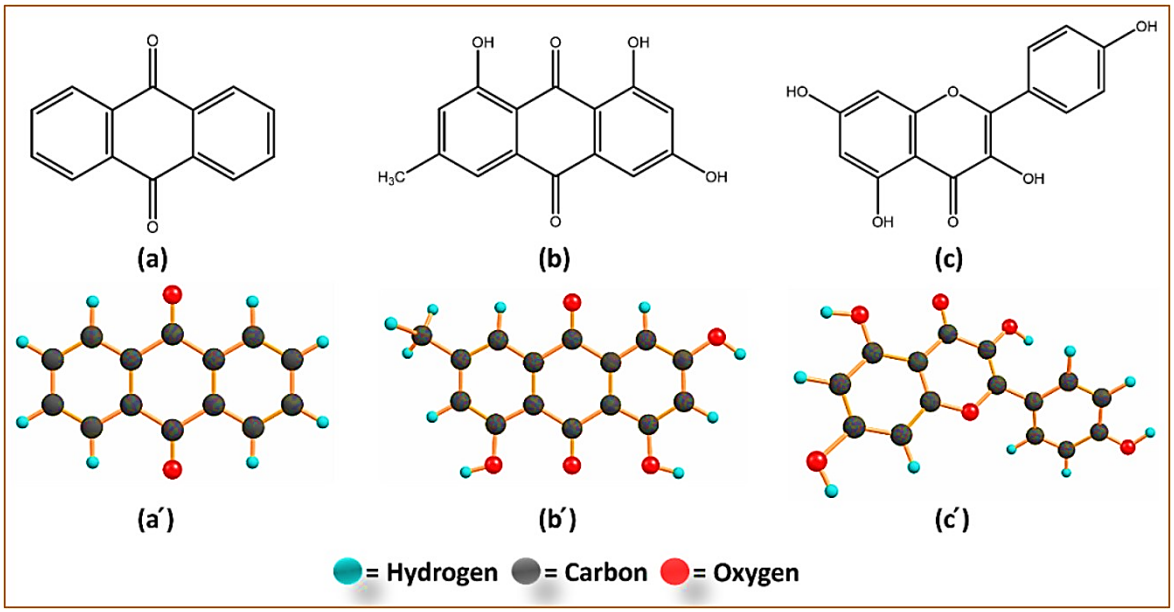

Figure 1: ChemDraw and Optimized structures of compound 1 (a) and (a′) Anthraquinone, compound 2 (b) and (b′) Emodin, and compound 3 (c) and (c′) Kaempferol.

Table 2: Toxicity of Compounds 1, 2 and 3.

Toxicity	Compound 1	Compound 2	Compound 3
hERG blockers	0.041	0.039	0.07
H-HT	0.077	0.046	0.098
DILI	0.855	0.935	0.979
AMES Toxicity	0.734	0.823	0.672
Rat Oral Acute Toxicity	0.134	0.096	0.156
FDAMDD	0.375	0.916	0.109
Skin Sensitization	0.142	0.678	0.856
Carcinogenicity	0.901	0.301	0.097
0Eye Corrosion	0.004	0.005	0.009
Eye Irritation	0.986	0.961	0.929
Respiratory Toxicity	0.043	0.076	0.09

Table 3: **The binding affinity (kcal/mol) of quercetin and kaempferol ligands with receptor 5L2S is evaluated through 9 different docking poses.**

Docking Pose	Compound 1	Compound 2	Compound 3
Pose 1	-8.8	-9.0	-8.5
Pose 2	-8.8	-8.6	-8.1
Pose 3	-8.8	-8.5	-7.9
Pose 4	-8.7	-8.5	-7.8
Pose 5	-8.3	-8.5	-7.4
Pose 6	-8.3	-8.4	-7.2
Pose 7	-8.3	-8.3	-7.2
Pose 8	-7.9	-8.2	-7.1
Pose 9	-7.5	-8.1	-6.9

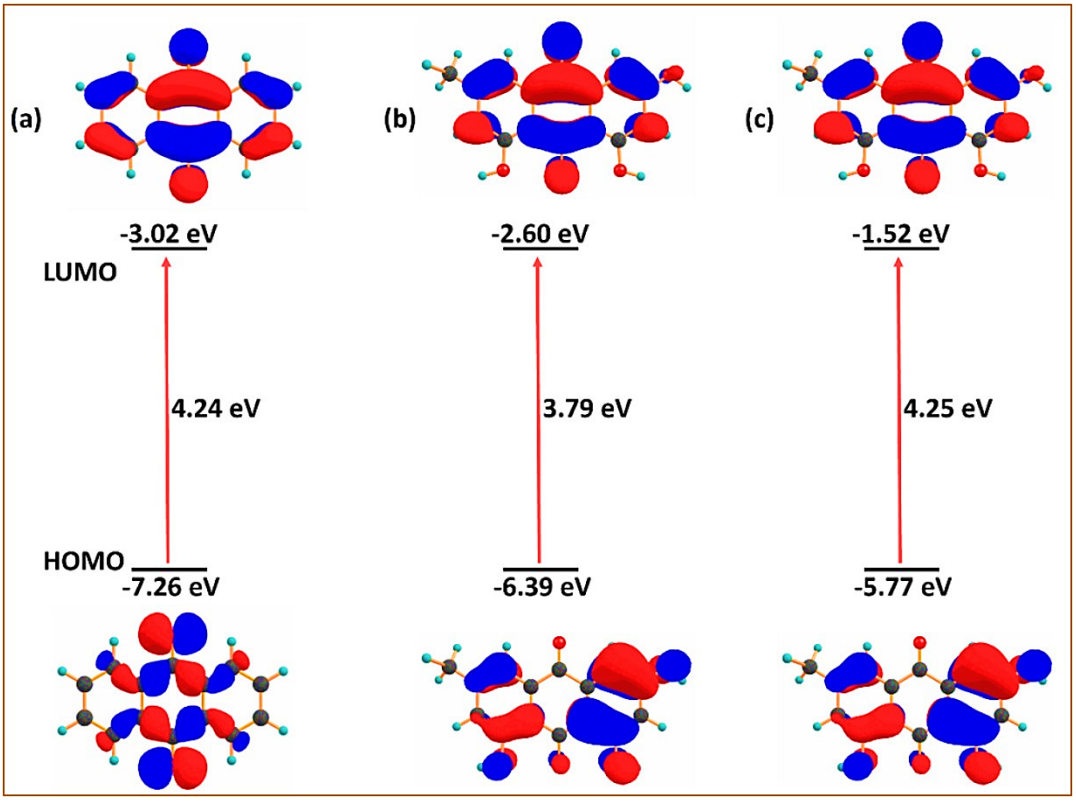

Figure 2: Frontier molecular orbital of (a) compound 1, Anthraquinone, (b) compound 2, Emodin, and (c) compound 3, Kaempferol.

Figure 6 shows the binding interactions of compounds 1, 2, and 3 within the active site of the target protein. Each ligand is stabilized by a network of non-covalent interactions that define its binding affinity and orientation inside the pocket.

For compound 1, stabilization is achieved through van der Waals forces with residues such as GLN A:149, ALA A:41, and PHE A:98, along with π-π stacking and π-alkyl interactions involving (TYR A:26=4.98Å) and (ALA A:162=5.35Å). These contacts help anchor the ligand firmly within the binding pocket (see Figure 6 (a)). Compound 2 shows a broader interaction network, including hydrogen bonds with GLN A:149 and ASP A:163, as well as van der Waals and hydrophobic contacts with residues like ILE A:19, VAL A:27, and ALA A:162. Additional π-σ (LEU A:152=3.99Å) and π-alkyl (ALA A:162=4.43Å) interactions further reinforce the stability of this complex (see Figure 6 (b)). The compound 3 forms hydrogen bonds with ASN A:150, ASP A:163 residues and π-anion (ASP A:163=3.92Å) and π-alkyl (ALA A:162=5.04Å) with aromatic hydrophobic residues, respectively (Figure 6(c)). It is stabilized by van der Waals contacts to PHE A:98, LEU A:152 and VAL A:27. Overall, the interaction maps reveal how each ligand easily fits and orients within a favourable position into the protein active pocket. Compound 2, which has multiple hydrogen bonds and a large number of hydrophobic contacts, is the most strongly stabilized; however, compounds 1 and 3 are also well-fitted due to the π-mediated and van der Waals contributions. This implies that the three ligands can bind and are bound with different degrees of affinity and rigidity.

DISCUSSION

The comparative analysis of compound 1 (Anthraquinone), compound 2 (Emodin) and compound 3 (Kaempferol) offers a deep understanding of the electronic, physicochemical and biological properties. FMO analysis indicates that these compounds have different electronic properties, potentially leading to differences in their reactivity as well as stability (Roy *et al.*, 2016; M. J. Frisch *et al.*, 2016). The energy gaps imply that Emodin (2) has a relatively smaller value of energy gap of 3.79 eV, making it a higher electronic excitation and reactivity than Anthraquinone (1, 4.24 eV) and Kaempferol (3, 4.25 eV).

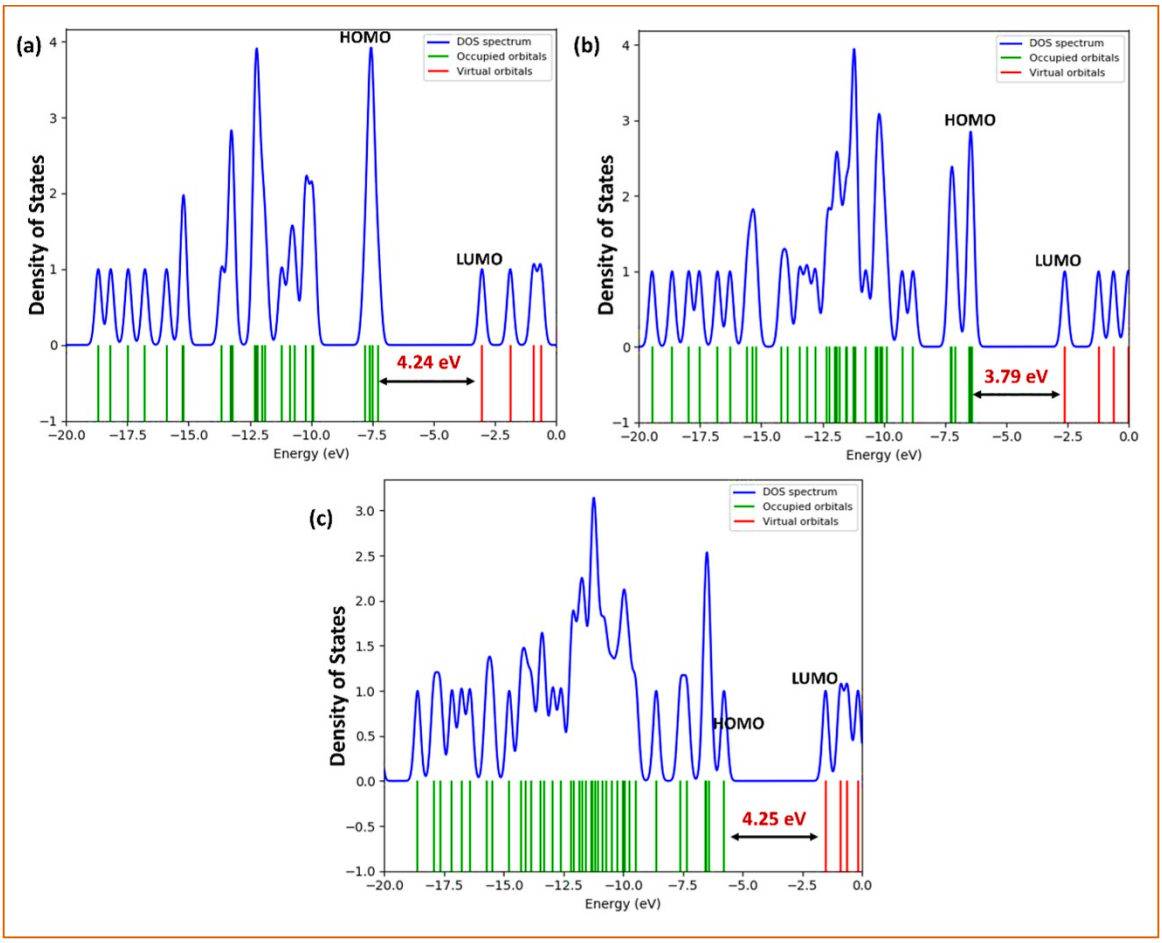

Figure 3: Density of states graphs of (a) compound 1, Anthraquinone, (b) compound 2, Emodin, and (c) compound 3, Kaempferol.

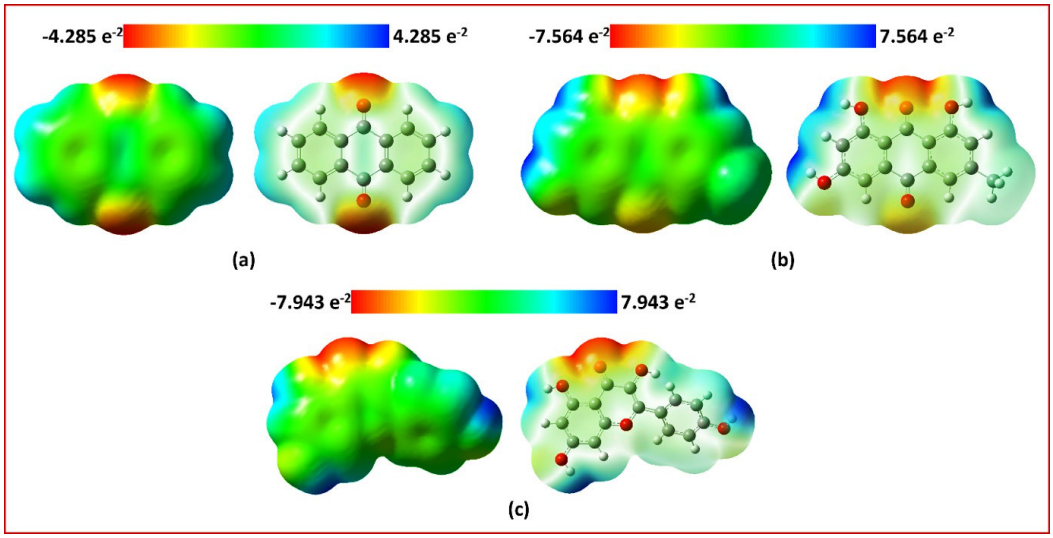

Figure 4: MEP maps of (a) compound 1, Anthraquinone, (b) compound 2, Emodin, and (c) compound 3, Kaempferol.

These also show that the narrower energy band gap in Emodin has enhanced capabilities for charge transfer. The larger gap in compounds 1 and 3 represents higher kinetic stability, but lower electron transfer efficiency. These observations can also be verified from DOS plots, in which compound 2 has the highest local electronic states in the vicinity of the Fermi level due to a denser population of electronic states near the Fermi resulting in easier excitation, and compounds 1 and 3 have occupied unoccupied orbitals well separated emphasizing the stability. This trend was further confirmed by the MEP maps analysis, which offers a visual representation of charge distribution and the potential reactive sides (Gu *et al*., 2024; Abuhejail *et al*., 2024; Rezvan *et al*., 2025). It has an intermediate reactivity because it possesses a relatively even distribution of electron density on the aromatic ring. In contrast, such intense red areas are observed for emodin, around which oxygen atoms and that, corresponds to a very electron-rich centre available for electrophilic attack. The kaempferol with the highest electronegative potential, because of polymethoxy and polyhydroxy groups that favour its ability to make hydrogen bonds and to coordinate metals. The higher electronegative potential from 1 (-4.285 e^{-2}) to 3 (-7.943 e^{-2}) is indicative of the increasing polarity and likely reactivity towards electrophilic species.

The pharmacokinetic study, combined with ADMET analysis, provides a realistic perspective on the *in vivo* molecular behaviour of these compounds. Anthraquinone, being the smallest and most lipophilic molecule, exhibits the best membrane permeability and blood-brain barrier penetration, potentially allowing it to achieve a desired CNS-targeted effect. However, its low polarity (TPSA=34.14) also indicates limited aqueous solubility. Emodin shows a profile with medium polarity, moderate balance and thus reasonable oral bioavailability, but low permeability, suggesting that it may have good circulation in the plasma yet not easily pass through lipid barriers. Kaempferol (TPSA=111.13) of the highest polarity possesses better solubility and hydrogen-bonding ability but decreased permeability, which may preclude it from reaching the intracellular site of action. All three compounds display high plasma protein binding (>97%), although Kaempferol presents the highest fraction unbound, with more free molecules available for biological effects. Metabolic profiling emphasises that all these compounds interact with cytochrome P450 enzymes, and particularly compound 3 (Kaempferol) has a stronger inhibitory effect against the CYP2D6 and CYP3A4, which reflects the possibility of drug-drug interactions. With respect to clearance, Anthraquinone is cleared rapidly, and Kaempferol stays longer because of a higher half-life, suggesting prolonged systemic retention.

The toxicity is very important for the safety profile information. All three compounds have very low hERG inhibitory activity, indicating that they may possess little risk of cardiotoxic. Nevertheless, liver toxicity becomes a major issue, in particular for Kaempferol, which has the highest DILI probability of 0.979.

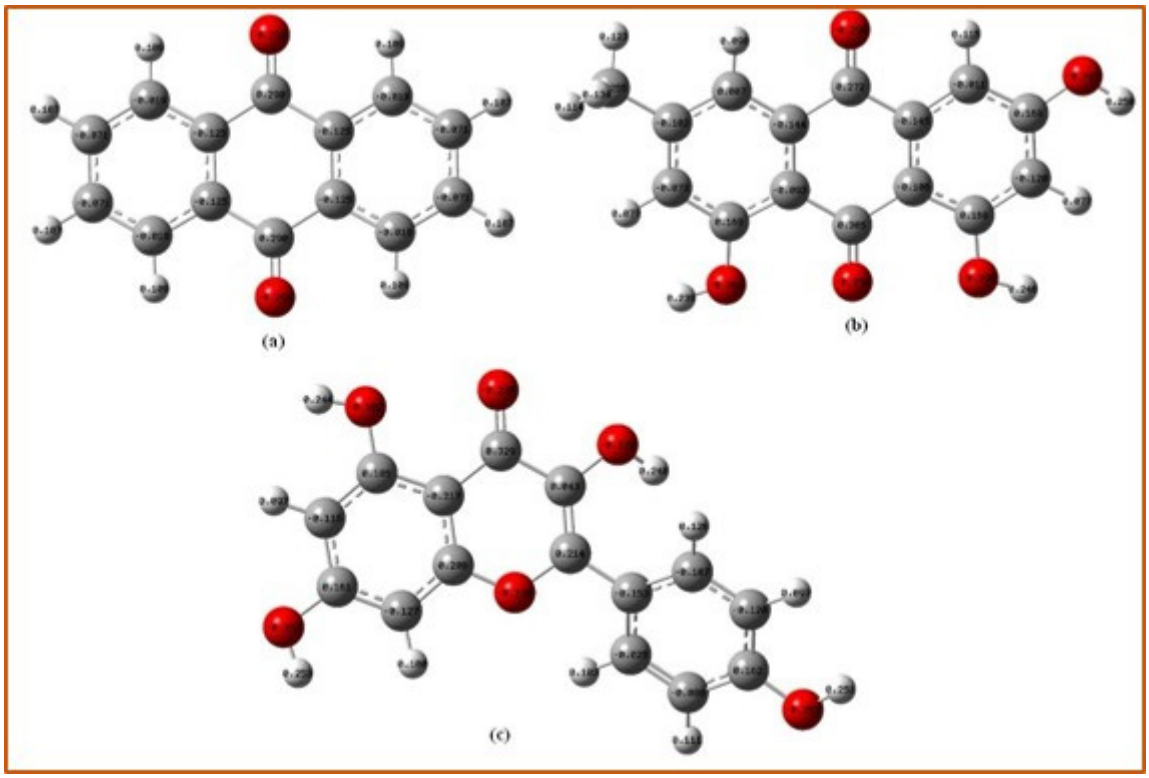

Figure 5: Mulliken charge distribution of (a) compound 1, Anthraquinone, (b) compound 2, Emodin, and (c) compound 3, Kaempferol.

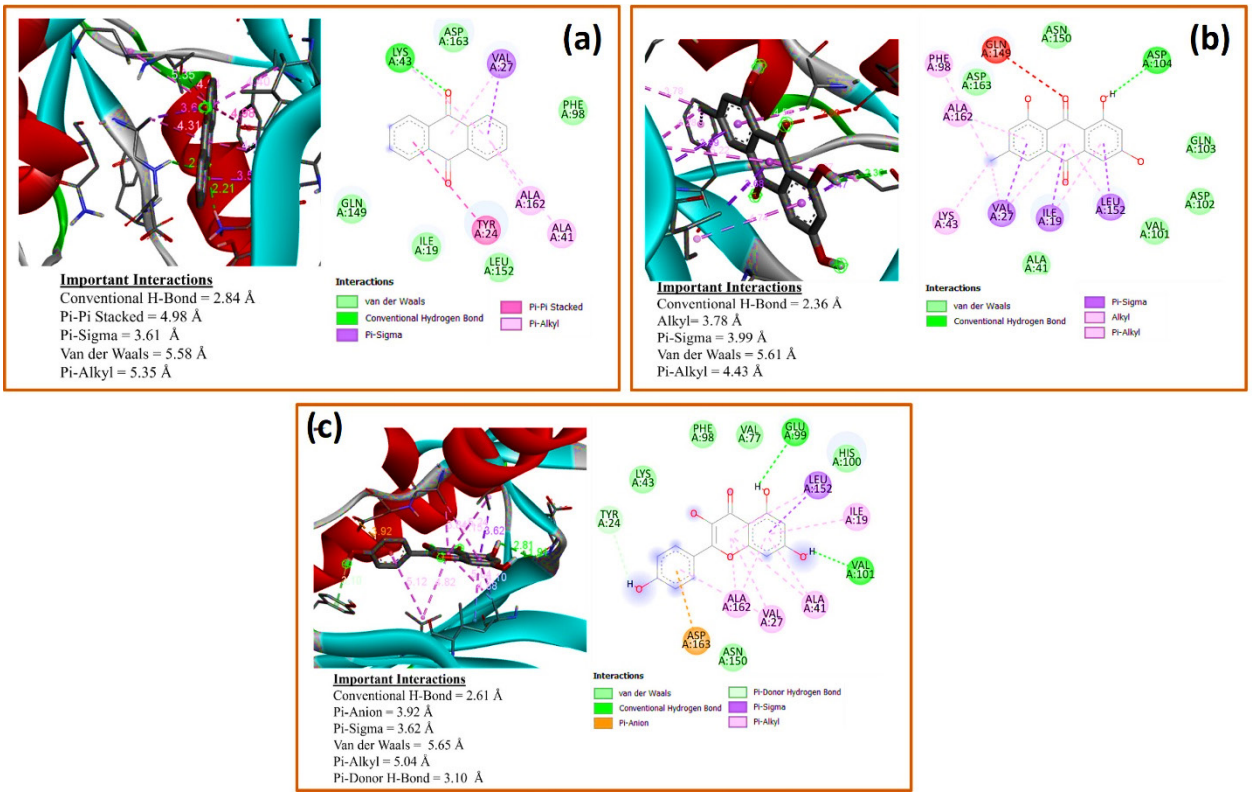

Figure 6: Docked structure of (a) compound 1, Anthraquinone, (b) compound 2, Emodin, and (c) compound 3, Kaempferol with 5L2S receptor (3D docked view, interactions with bond lengths and 2D interaction diagram).

Emodin is more mutagenic, Anthraquinone may have a lower hepatic risk, but has higher carcinogenicity potential (0.901) and would be more likely to cause eye irritation. These results emphasize the fine line between bioactivity and safety: enhanced reactivity and bioavailability are generally associated to greater toxicity levels. Therefore, a high reactivity of Emodin might be beneficial for biological interactions and concurrent genotoxic and hepatotoxic risks. Kaempferol has a long-acting effect, which enhances the efficacy far beyond Antagonistic potency; however, liver toxic risk is increased. Anthraquinone's stable action makes it safe in pharmacological applications, but it may produce carcinogenic potential.

Molecular docking calculations of the compounds toward the CDK6 receptor (PDB 5L2S) further reveal details about biological activity. Emodin shows the best and largest binding affinity, by docking scores from -9.0 to -8.1 kcal mol^{-1} with two or three hydrogen bonds and π-π stacking effects on crucial residues such as GLN A:149and ASP A:163. Anthraquinone also exhibits strong (and stable) interactions (-8.8 to -7.5 kcal mol^{-1}), mostly relying on π-π and van der Waals contacts, suggesting a reliable binding, although less flexible. Kaempferol, although with a somewhat lower affinity (-8.5 to -6.9 kcal mol^{-1}), remains bound to hydrogen bonds involving ASN A:150 and ASP A:163 and π-anion interactions.

CONCLUSION

We focused on three compounds, i.e., Anthraquinone (compound 1), Emodin (compound 2) and Kaempferol (compound 3), in our study, which were studied by the approach of DFT, ADMET predictions, toxicity profiling and molecular docking. FMO analysis indicated compound 2 is the most chemically reactive with the narrowest energy gap, and compounds 1 and 3 are more stable in comparison. MEP maps indicated oxygen-rich regions are the reactive sites, and compound 3 exhibited the most electronegative potential. The ADMET profile of compound 1 indicates good BBB penetration but rapid clearance and a high risk of carcinogenicity; the profile for compound 2 is associated with strong oral bioavailability and preferred pharmacokinetics, although increased mutagenicity and liver toxicity are observed, whereas the profile of compound 3 includes improved solubility together with a long half-life but modest CNS uptake. Docking studies confirmed that compound 2 was the most potent binder to CDK6 (5L2S) with several hydrogen bonds and hydrophobic interactions, while compounds 1 and 3 also exhibited strong and moderate binding behaviour, respectively, due to their reactive functional groups, which accelerate toxicity-related issues. Overall, compound 2 is predicted as the most promising CDK6 inhibitor scaffold despite safety concerns; compound 3 presents balanced reactivity and pharmacokinetics with moderate binding potential, whereas compound 1 shows partial therapeutic promise due to its safety profile.

ACKNOWLEDGEMENT

The author gratefully acknowledges Department, EXPRTESSMED Diagnostics and Research, Bahrain for their valuable support and encouragement.

ABBREVIATIONS

CDKs: Cyclin-dependent kinases; **ROS:** Reactive oxygen species; **DFT:** Density functional theory; **DOS:** Density of states; **FMO:** Frontier Molecular Orbital; **HOMO:** Highest Occupied Molecular Orbital; **LUMO:** Lowest Unoccupied Molecular Orbital; **HIA:** Human intestinal absorption; **TPSA:** Total polar surface area; **VD:** Volume distribution; **Fu:** Fraction unbound; **H-HT:** Human risk for hepatotoxicity; **DILI:** Drug-induced liver injury; **FDAMDD:** FDA maximum recommended daily dose; **MEP:** Molecular Electrostatic Potential.

CONFLICT OF INTEREST

The authors declare that there is no conflict of interest.

GENERATIVE AI STATEMENT

The author declares that generative AI (Artificial Intelligence) tools, including Grammarly and QuillBot, were used to enhance the language and clarity of this work. The author takes full responsibility for the accuracy and integrity of the content.

SUMMARY

This study computationally evaluated Anthraquinone (1), Emodin (2), and Kaempferol (3) using DFT, ADMET/toxicity profiling, and docking to CDK6 (5L2S). Emodin (2) showed the highest reactivity (smallest HOMO-LUMO gap) and the strongest docking affinity, but raised mutagenicity and hepatotoxicity concerns; Anthraquinone (1) exhibited BBB penetration yet rapid clearance and carcinogenic risk, while Kaempferol (3) displayed high electronegative potential, better solubility, and the longest half-life with modest CNS uptake and moderate binding. Overall, Emodin is the leading CDK6 inhibitor scaffold despite safety flags, Kaempferol offers a more balanced profile, and Anthraquinone is limited mainly by predicted toxicity.

AUTHOR CONTRIBUTIONS

Israa Jameel Hakeem and Qamre Alam conducted the data analysis, designed the experiment, and wrote the final draft. Shahnaz Haque and Misbahuddin Rafeeq contributed to writing the Discussion and Results sections. Mohammad Azhar Kamal and Tahani Bakhsh wrote the review, conducted the literature search, and interpreted the data. Abdulrahman Almutairi, Rashed Ahmed Alniwaider, and Ali Bin Thani prepared the initial manuscript draft.

REFERENCES

Abuhejail, R. M., Radwan, A. A., Alzoman, N. Z., and Darwish, I. A. (2024). Formation and characterization of charge transfer complex between alectinib and 2,3-dichloro-5,6-dicyano-1,4-benzoquinone: Application to development of microwell spectrophotometric method. Sustainable Chemistry and Pharmacy, 39, 101524.

Allouche, A.-R. (2012). Gabedit: A Graphical User Interface for Computational Chemistry Softwares. Journal of Computational Chemistry, 32, 174-182.

Andrades-Lagos, J., Campanini-Salinas, J., Pedreros-Riquelme, A., Mella, J., Choquesillo-Lazarte, D., Zamora, P. P., Pessoa-Mahana, H., Burbulis, I., and Vásquez-Velásquez, D. (2023). Design, Synthesis, and Structure-Activity Relationship Studies of New Quinone Derivatives as Antibacterial Agents. Antibiotics (Basel), 12(6), 1065.

Becke, A. D. (1993). Density-functional Thermochemistry. III. The Role of Exact Exchange. Journal of Chemical Physics, 98, 5648-5652.

BIOVIA, Dassault Systèmes. (2021). BIOVIA Discovery Studio [Software]. San Diego: Dassault Systèmes. https://www.3ds.com/products/biovia/discovery-studio

Dennington, R., Keith, T. A., and Millam, J. M. (2016). GaussView, Version 6.1 [Software]. Shawnee Mission, KS: Semichem Inc.

Ding, L., Cao, J., Lin, W., Chen, H., Xiong, X., Ao, H., Yu, M., Lin, J., and Cui, Q. (2020). The Roles of Cyclin-Dependent Kinases in Cell-Cycle Progression and Therapeutic Strategies in Human Breast Cancer. International Journal of Molecular Sciences, 21(6), 1960.

El-Kasaby, R. A., Al-Farraj, E. S., Abdou, A., and Abu-Dief, A. M. (2025). Synthesis, Spectral Analysis, physicochemical investigation and biomedical potential of some Novel Cu(II), Ru(III) and VO(II) Complexes with Anthraquinone-Based Schiff Base supported by DFT and Molecular Docking Insights. Journal of Molecular Structure, 1345, 143010.

Frisch, M. J., Pople, J. A., and Binkley, J. S. (1984). Self-consistent Molecular Orbital Methods 25. Supplementary Functions for Gaussian Basis Sets. Journal of Chemical Physics, 80, 3265-3269.

Frisch, M. J., Trucks, G. W., Schlegel, H. B., Scuseria, G. E., Robb, M. A., Cheeseman, J. R., Scalmani, G., Barone, V., Petersson, G. A., Nakatsuji, H., Li, X., Caricato, M., Marenich, A. V., Bloino, J., Janesko, B. G., Gomperts, R., Mennucci, B., Hratchian, H. P., Ortiz, J. V., Izmaylov, A. F., Sonnenberg, J. L., Williams-Young, D., Ding, F., Lipparini, F., Egidi, F., Goings, J., Peng, B., Petrone, A., Henderson, T., Ranasinghe, D., Zakrzewski, V. G., Gao, J., Rega, N., Zheng, G., Liang, W., Hada, M., Ehara, M., Toyota, K., Fukuda, R., Hasegawa, J., Ishida, M., Nakajima, T., Honda, Y., Kitao, O., Nakai, H., Vreven, T., Throssell, K., Montgomery, J. A., Jr., Peralta, J. E., Ogliaro, F., Bearpark, M. J., Heyd, J. J., Brothers, E. N., Kudin, K. N., Staroverov, V. N., Keith, T. A., Kobayashi, R., Normand, J., Raghavachari, K., Rendell, A. P., Burant, J. C., Iyengar, S. S., Tomasi, J., Cossi, M., Millam, J. M., Klene, M., Adamo, C., Cammi, R., Ochterski, J. W., Martin, R. L., Morokuma, K., Farkas, O., Foresman, J. B., and Fox, D. J. (2016). Gaussian 16, Revision A.03 [Software]. Wallingford, CT: Gaussian, Inc.

Gu, J., Wang, T., Song, Y., and Ma, J. (2024). Catalysis of first triplet p-benzoquinone for electron ejection from sulfite: Significance of single electron transfer. Chemical Engineering Journal, 494, 152962.

Lee, C., Yang, W., and Parr, R. G. (1988). Development of the Colle Salvetti Correlation-Energy Formula into a Functional of the Electron Density. Physical Review B, 37, 785-789.

Lukasik, P., Załuski, M., and Gutowska, I. (2021). Cyclin-Dependent Kinases (CDK) and Their Role in Diseases Development-Review. International Journal of Molecular Sciences, 22(6), 2935

Lu, J.-X., Lan, H.-R., Zeng, D., Song, J.-Y., Hao, Y.-T., Xing, A.-P., Shen, A., and Yuan, J. (2025). Design, synthesis, anticancer activity and molecular docking of quinoline-based dihydrazone derivatives. RSC Advances, 15, 231-243.

Mariam, Y. H., and Sawyer, A. (1996). A computational study on the relative reactivity of reductively activated 1,4-benzoquinone and its isoelectronic analogs. Journal of Computer-Aided Molecular Design, 10(5), 441-460.

Meem, M. H., Yusuf, S. B., Al Abbad, S. S., Rahman, S., Al-Gawati, M., Albrithen, H., Alodhayb, A. N., and Uddin, K. M. (2024). Exploring the anticancer and antibacterial potential of naphthoquinone derivatives: a comprehensive computational investigation. Frontiers in Chemistry, February 2024.

Moussaoui, M., Baassi, M., Baammi, S., Soufi, H., Salah, M., Daoud, R., and Belaaouad, S. (2023). In silico design of novel CDK2 inhibitors through QSAR, ADMET, molecular docking and molecular dynamics simulation studies. Journal of Biomolecular Structure and Dynamics, 41(23), 13646-13662.

Muraleedharan, K. (2024). Possible NLO response and electrical/charge transfer capabilities of natural anthraquinones as p-type organic semiconductors: a DFT approach. Journal of Molecular Modeling, 30.

Pellarin, I., Dall'Acqua, A., Favero, A., *et al.* (2025). Cyclin-dependent protein kinases and cell cycle regulation in biology and disease. Signal Transduction and Targeted Therapy, 10, 11.

Rathod, S., Shinde, K., Porlekar, J., Choudhari, P., Dhavale, R., Mahuli, D., Tamboli, Y., Bhatia, M., Haval, K. P., Al-Sehemi, A. G., and Pannipara, M. (2022). Computational Exploration of Anti-cancer Potential of Flavonoids against Cyclin-Dependent Kinase 8: An In Silico Molecular Docking and Dynamic Approach. ACS Omega, 8(1), 391-409.

Rezvan, V. H., and Salehzadeh, J. (2025). Exploring Charge Transfer Complexes of Fluoroquinolone Drugs and π-Acceptors (Picric Acid and 3,5-Dinitrobenzoic Acid): DFT Insights into Electronic Interactions, Thermodynamic Stability, FMOs, and NLO Properties. ChemistrySelect, 10.

Sadeghian, Z., Bayat, M., and Gheidari, D. (2025). Synthesis, molecular docking, pharmacological evaluation, MD simulation, and DFT calculations of quinazolin-12-one derivatives as PDK1 inhibitors. Nanoscale Advances, 7, 5760-5783.

Sharma, M., Savita, S., Wadhwa, K., Mishra, V., Javed, S., Ranjan, K. R., Rathi, A. K., and Kaur, H. (2025). Experimental, Spectroscopic Analysis, DFT and Molecular Docking studies of Pyridine based biologically active anti-fungal drug derivative of para-benzoquinone and benzimidazole. Journal of Molecular Structure, 1338, 142212.

Trott, O., and Olson, A. J. (2009). AutoDock Vina: Improving the Speed and Accuracy of Docking with a New Scoring Function, Efficient Optimization, and Multithreading. Journal of Computational Chemistry, 31(2), 455-461.

Valarmathi, T., Premkumar, R., Jebaseelan, J., and Franklin, M. (2023). Spectroscopic Characterization, Quantum Chemical and Molecular Docking Studies on 1-Chloroanthraquinone: A Novel Oral Squamous Cell Carcinoma Drug. Polycyclic Aromatic Compounds, 44, 1816-1834.

White, N. J., Tunstall, W. W., Vargas, L. A., Workman, K. T., Moldenhauer, J., and Gichuhi, W. K. (2025). Benzoquinone, 1,4-naphthoquinone radical anions, and their didehydro derivatives: electroanalytical and predicted negative ion photoelectron spectroscopic studies. Physical Chemistry Chemical Physics, 27, 8976-8993.

Xiong, G., Wu, Z., Yi, J., Fu, L., Yang, Z., Hsieh, C., Yin, M., Zeng, X., Wu, C., Lu, A., Chen, X., Hou, T., and Cao, D. (2021). ADMETlab 2.0: An Integrated Online Platform for Accurate and Comprehensive Predictions of ADMET Properties. Nucleic Acids Research, 49(1), W5-W14.

Zhou, X., Khetan, A., and Er, S. (2021). Evaluation of Computational Chemistry Methods for Predicting Redox Potentials of Quinone-Based Cathodes for Li-Ion Batteries. Batteries, 7, 71.

Cite this article: Hakeem IJ, Haque S, Rafeeq M, Kamal MA, Bakhsh T, Almutairi A, Alniwaider RA, *et al*. Integrative Computational Analysis of Bioactive Benzoquinones: CDK Binding, Toxicity, and Pharmacokinetics. Int. J. Pharm. Investigation. 2026;16(3):1183-93.